RSC Advances

RSC Advances

www.rsc.org/advances

This is an *Accepted Manuscript*, which has been through the Royal Society of Chemistry peer review process and has been accepted for publication.

Accepted Manuscripts are published online shortly after acceptance, before technical editing, formatting and proof reading. Using this free service, authors can make their results available to the community, in citable form, before we publish the edited article. This *Accepted Manuscript* will be replaced by the edited, formatted and paginated article as soon as this is available.

You can find more information about *Accepted Manuscripts* in the **Information for Authors**.

Please note that technical editing may introduce minor changes to the text and/or graphics, which may alter content. The journal's standard **Terms & Conditions** and the **Ethical guidelines** still apply. In no event shall the Royal Society of Chemistry be held responsible for any errors or omissions in this *Accepted Manuscript* or any consequences arising from the use of any information it contains.

ROYAL SOCIETY OF CHEMISTRY

www.rsc.org/advances

Please do not adjust margins

RSC Advances

Journal Name

ARTICLE

Porous Organic Polymers Derived from Tetrahedral Silicon-Centered Monomers and Stereocontorted Spirobifluorene-Based Precursor: Synthesis, Porosity and Carbon Dioxide Sorption†

Qing-Yu Ma,[a,b,]* Bing-Xue Yang[a,b] and Jian-Quan Li[a,b]

Sonogashira-Hagihara coupling reactions of tetrahedral silicon-centered monomers, i.e., tetrakis(4-bromophenyl)silane (p-Si) and tetrakis(3-bromophenyl)silane (m-Si), and stereocontorted 2,2',7,7'-tetraethynyl-9,9'-spirobifluorene (TESF) result in two novel porous organic polymers, POP-1 and POP-2. Compared with other porous polymers, these materials show high thermal stability and comparable specific surface area with Brunauer-Emmer-Teller surface areas of up to 983 $m^2\,g^{-1}$, and total pore volume of up to 0.81 $cm^3\,g^{-1}$ (POP-1). The N_2 isotherm analysis reveals that their porosities could be tuned by changing the structure geometry of silicon-centered monomers. Further porosity comparison with other porous polymers indicates that the introduction of silicon-centered units in the porous networks could increase the porosity and copolymerization, i.e., changing the second monomer, is an efficient strategy to tune the porosity of the final materials. For applications, the resulting materials show moderate carbon dioxide uptakes of up to 1.92 mmol g^{-1} (8.45 wt%) at 273 K and 1.03 bar, and 1.12 mmol g^{-1} (4.93 wt%) at 298 K and 1.01 bar (POP-1), and also a comparably high binding ability with CO_2 with isostreic heat of 26.8 kJ mol^{-1} (POP-1). Moreover, the materials exhibited moderate selectivity of CO_2 over other gases, including N_2, O_2 and CH_4. These results reveal that these materials could be potentially applied as promising candidates for storing and capturing CO_2.

Introduction

In recent years, the design and construction of porous organic polymers (POPs) have attracted significant interest of scientists because of their extensively potential applications in the areas of gas storage, separation, heterogeneous catalysis and sensor, *etc*.[1-6] POP materials are often prepared via the direct synthesis methodology because this approach has characteristic advantages: a high utilization efficiency of the starting materials and facile formation of micropores.[3] In this methodology, two important issues should be addressed. One is selecting proper chemical synthesis methods to efficiently link the building blocks together over a broad range. Among various methods, Sonogashira-Hagihara reaction is a typical class of routes and has been well established for the synthesis of POP materials,[7-9] especially conjugated microporous polymers (CMPs), which combine microporosity and π-conjugated bond and have a great promise in the range of applications such as light-harvesting, photocatalysis and

sensing, except the typical usage in gas storage.[10] Another is the choice of the correct monomers, which are crucial to the formation of porous networks with adequate stability and largely influence the various properties of the final products. The monomers are generally selected to be rigid or contorted as well as having multifunctional reaction sites. It has been proved that monomers with diversified geometries such as linear,[11] planar,[12] tetrahedral,[13] and octahedral geometries[14] can meet the demand of rigidity or contortion and thus easily afford the porosity. Additionally, linking the monomers with different geometries could combine their advantages and further tune the porosity and functionality of the resulting polymers.[15]

In terms of selecting suitable monomers, tetrahedral or stereocontorted monomers have been considered as ideal options because enhanced surface area and porosity could be easily achieved by introducing these monomers as building blocks, which can lack the flexibility to pack efficiently resulting in facile formation of free volumes to promote the porosity.[1-3,16] For example, a microporous polymer, PAF-1, derived from a typical tetrahedral monomer, tetrakis(4-bromophenyl) methane, showed an ultrahigh Brunauer-Emmett-Teller (BET) surface area of 5600 $m^2\,g^{-1}$ as well as high physicochemical stability.[17] Compared with other tetrahedral units, silicon-based monomers have attracted particular interest of researchers because of their unique characteristics. In general, the synthesis procedures of silicon-centered monomers are more accessible than their carbon equivalents. Silicon-

[a.] *Shandong Provincial Key Laboratory of Preparation and Measurement of Building Materials, University of Jinan, Jinan 250022, Shandong, China*
[b.] *School of Materials Science and Engineering, University of Jinan, Jinan 250022, Shandong, P. R. China. Corresponding author: mse_maqy@ujn.edu.cn, Tel: +86 531 89736751; Fax: +86 531 82523518.*

RSC Advances Accepted Manuscript

centered units possess greater flexibility than the carbon analogs due to longer bond length and increased bond angel of silicon and thus could affect strain and hence supramolecular geometry.[18] Furthermore, POP materials derived from silicon-based monomers may exhibit higher surface area than those from carbon analogs.[13,19-21] For example, by replacing tetrakis (4-bromophenyl)methane with tetrakis(4-bromophenyl)silane, Zhou *et al.* reported a porous polymer with an unprecedented high BET surface area of up to 6461 m^2 g^{-1}, which represents the highest BET surface area of porous materials to date.[13] Additionally, introducing silicon-centered units in the porous networks, their optical and electronic properties can be also tuned because of the electron-releasing nature of silicon atom.[15]

Meanwhile, stereocontorted spirobifluorene monomers are continuously being developed to fabricate POP materials because the spirobifluorene unit introduces a kink into each repeating unit, thus preventing efficient packing.[1-3] For instance, a number of spirobifluorene-based POP materials have been prepared from 2,2',7,7'-tetrabromo-9,9'-spirobifluorene (TBSF) by homo- or co- polymerization reaction.[22,23] It is worthy to note that the resulting porosity could be tuned not only by the choice of monomers but also by the synthetic routes and reaction conditions. For example, copolymerization of TBSF with 1,4-dibromobenzene by Yamamoto reaction yielded a network with higher surface area (887 m^2 g^{-1}) than TBSF with 1,4-diboronic acid (450 m^2 g^{-1}) and 1,4-diethynyl anologues (510 m^2 g^{-1}) by Suzuki reaction and Sonogashira-Hagihara reaction, respectively.[22,23] Although silicon-centered monomers and spirobifluorene-based monomers play an important role in the construction of POP materials, to the best of our knowledge, there is no report on the exploration of POP materials containing both of these two kinds of monomers.

In the present study, we combined the advantages of tetrahedral silicon-centered monomers and spirobifluorene-based precursors, and simultaneously utilized them to construct two novel porous organic polymers, POP-1 and POP-2, using two common silicon-centered compounds, i.e., tetrakis(4-bromophenyl)silane (*p*-Si) and tetrakis(3-bromophenyl)silane (*m*-Si), and 2,2',7,7'-tetraethynyl-9,9'-spirobifluorene (TESF) as the building blocks via Sonogashira-Hagihara coupling reaction (see Scheme 1). As expected, the resulting materials showed high porosities and thermal stability. Their porosities could be tuned by altering the structure geometry of the silicon-containing units. Moreover, their applications in carbon dioxide (CO_2) sorption and the selectivity of CO_2 over other gases were explored.
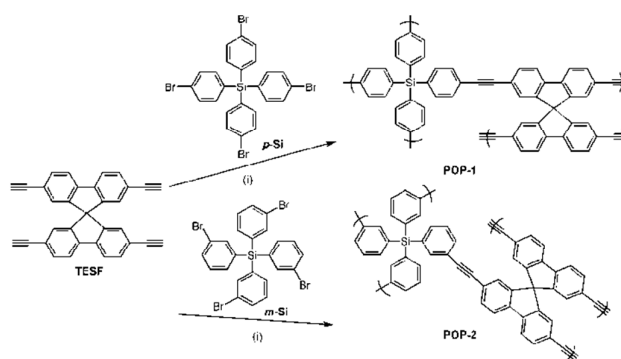
Scheme 1 Synthetic routes of porous organic polymers, POP-1 and POP-2. (i): Pd(PPh$_3$)/CuI, DMF/*i*-Pr$_2$NH, 90°C, 72h. The fragments of these porous polymers are shown as examples.

Experimental

Materials

Unless otherwise noted, all reagents were obtained from commercial suppliers and used without further purification. 2,2',7,7'-Tetraethynyl-9,9'-spirobifluorene (TESF),[24] tetrakis(4-bromophenyl)silane (*p*-Si)[25] and tetrakis(3-bromophenyl)silane (*m*-Si)[26] were synthesized by the previous reports. *N,N*-dimethylformamide (DMF) was first dried over CaH$_2$ at 80°C for 12 h and distilled under vacuum pressure. Then DMF was stored with 4 Å molecule sieves prior to use. Triethylamine (*i*-Pr$_2$NH) was dried over CaH$_2$ and used freshly.

Characterization

Fourier transform infrared (FT-IR) spectra of the products were recorded on a Bruker Tensor27 spectrophotometer. Solid-state ^{13}C cross-polarization/magic-angle-spinning (CP/MAS) NMR and ^{29}Si MAS NMR spectra were performed on Bruker AVANCE-500 NMR Spectrometer operating at a magnetic field strength of 9.4 T. The resonance frequencies at this field strength were 125 and 99 MHz for ^{13}C NMR and ^{29}Si NMR, respectively. A chemagnetics 5 mm triple-resonance MAS probe was used to acquire ^{13}C and ^{29}Si NMR spectra. ^{29}Si MAS NMR spectra with high power proton decoupling were recorded using a π/2 pulse length of 5 μs, a recycle delay of 120 s and a spinning rate of 5 kHz. Elemental analyses were evaluated using an Elemental vario EL III elemental analyzer.

Field-emission scanning electron microscopy (FE-SEM) experiments were performed by using HITACHI S4800 Spectrometer. Thermogravimetric analyses were performed with a MettlerToledo SDTA-854 TGA system in nitrogen at a heating rate of 10°C min^{-1} to 800°C.

Nitrogen (N_2) sorption isotherm measurements were performed on a Micro Meritics surface area and pore size analyzer. Before measurement, samples were degassed at 150°C for least 12 h. A sample of ca. 100 mg and a UHP-grade nitrogen (99.999%) gas source were used in the nitrogen sorption measurements at 77 K and collected on a Micromeritics ASAP 2020 volumetric adsorption analyzer. BET surface areas were determined over a P/P_0 range from 0.01 to

0.20. Nonlocal density functional theory (NL-DFT) pore size distributions were determined using the carbon/slit-cylindrical pore mode of the Quadra win software. Carbon dioxide (CO_2) adsorption and desorption isotherms at 298 K and 273 K, and N_2, methane (CH_4) and oxygen (O_2) adsorption isotherms at 298 K were measured on a Micrometrics ASAP 2020 volumetric adsorption analyzer. Prior to the measurements, the samples were degassed at 150 °C for at least 12 h.

Synthesis of porous organic polymers, POP-1 and POP-2

POP-1. TESF (0.38 g, 1.2 mmol), p-Si (0.52 g, 0.8 mmol), Pd(PPh$_3$)$_4$ (32 mg, 0.028 mmol), CuI (16 mg, 0.08 mmol) were added into a 25 mL three round-bottom flask charged with 5 ml of freshly distilled DMF and 5 ml of freshly distilled i-Pr$_2$NH. The solution was stirred for 72 h at 90°C under an atmosphere of argon. Then the mixture was cooled to room temperature, filtrated and washed with water, THF, methanol and acetone to remove any amine salts, unconsumed monomers and catalyst residues. Further purification of the crude products was conducted by exhaustive Soxhlet extraction with THF for 24 h and methanol for 24 h. The product was collected after being dried under vacuum at 70°C for 48 h and afforded as a dark brown solid (0.78 g, yield: 87%). Elemental analysis calc. (wt.%) for C$_{147}$H$_{68}$Si$_2$: C 93.4, H 3.6; Found C 76.61, H 4,43. The calculated yield and the contents of C and H were based on hypothetical 100% polycondensation between equivalent ethynyl and bromo- groups in the Sonogashira-Hagihara coupling reaction. Since the ethynyl functionality is excess, both of the two starting monomers are used to calculate the yield of each polymer.

POP-2. The synthesis procedure and post-treatment of POP-2 were similar to those of POP-1 except that p-Si was replaced by m-Si. POP-2 was afforded as a dark brown solid (0.81 g, yield: 90%). Elemental analysis calc. (wt.%) for C$_{147}$H$_{68}$Si$_2$: C 93.4, H 3.6; Found C 77.73, H 4.1. The calculated methods of yield and the contents of C and H for POP-2 were similar to those for POP-1.

Results and discussion

Synthesis and characterization

Scheme 1 shows the synthetic routes of porous organic polymers (POPs). The targeted polymers were synthesized through the direct (A$_4$+B$_4$) Sonogashira-Hagihara palladium-catalyzed coupling reactions of two silicon-based monomers, i.e., tetrakis(4-bromophenyl)silane (p-Si) and tetrakis(3-bromophenyl)silane (m-Si) with 2,2',7,7'-tetraethynyl-9,9'-spirobifluorene (TESF), yielding POP-1 and POP-2, respectively. For the reactions, we utilized a 1.5 M excess of ethynyl functionality and the reactions were carried out using Pd(PPh$_3$)/CuI as the catalyst system and i-Pr$_2$NH as the acid absorbent in DMF at 90°C for 72 h because it was shown to lead to higher porosity in the final materials as proved by Cooper, Kiskan and co-workers.[27,28] After the reactions, the crude products were recovered by filtration, washed and extracted with several solvents, and dried under vacuum at 70°C for 12 h to yield the materials. All the polymers were

obtained as dark brown solids. The final products were insoluble in common organic solvents including THF, DMF, acetone, methanol, and chemically stable in various aqueous conditions. Similar to other previous reports,[7-9,27] there are relatively large differences between the calculated and found contents of C and H by elemental analysis. This difference could be attributed to two aspects: i) incomplete reaction between ethynyl and bromo- groups while the calculated contents were based on hypothetical 100% polycondensation; and ii) the residual amine salts, solvents or catalysts in the final polymers because the residuals may be embedded in the porous networks, such as in the closed pores, and they were difficult to remove completely even after exhaustive Soxhlet extraction.

The structures of the resulting polymers were first characterized by FT-IR spectroscopy. As shown in Fig. 1, the intensity of characteristic terminal ethynyl hydrocarbon (-C≡CH) bond vibration peak at ca. 3310 cm^{-1} was very weak and covered by wide peak at ca. 3450 cm^{-1} of the –OH groups from water encapsulated in the samples. The characteristic peak of bis-substituted acetylene (-C≡C-) was also weak but can be observed at ca. 2210 cm^{-1}. These results indicate the successful process and high degree of the coupling reaction. The peaks from 1600 cm^{-1} to 1400 cm^{-1} with moderate intensity are attributed to the C=C stretching vibration of phenyl rings.
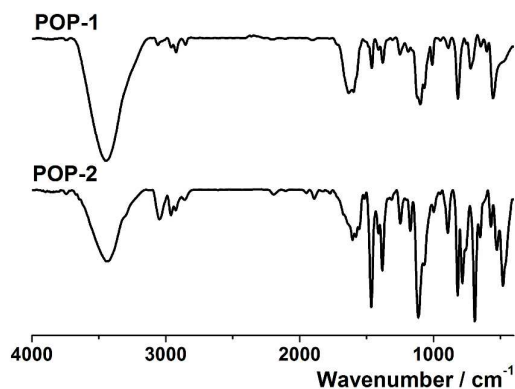

Fig. 1 FT-IR spectra of POP-1 and POP-2 (the wide peak around 3450 cm^{-1} is assigned to -OH group from water encapsulated in the samples)

Further identification of the local structures of the polymers was determined by solid-state ^{13}C CP/MAS NMR spectroscopy (Fig. 2). As expected, POP-1 and POP-2 showed similar spectrum. The sp^2 phenyl carbon atoms from phenylene and spirobifluorene units are observed from 120 ppm to 150 ppm. The ethynylene (-C≡C-) units were observed at ca. 90 ppm, confirming the formation of internal C-C triple bonds between the ethynyl units and brominated phenyl units. Resonances observed at ca. 67 ppm can be attributed to the quaternary carbon atom from the spirobifluorene units. Solid-state ^{29}Si CP/MAS NMR spectroscopy was also performed to determine the structures of tetrahedral silicon-centers. Only one major peak at −14.7 ppm and −15.5 ppm was observed for POP-1 and POP-2 (Fig. 3), which is obviously corresponding to Si(p-C$_6$H$_4$)$_4$ units and Si(m-C$_6$H$_4$)$_4$ units. These results agree with the

previous ^{29}Si NMR measurements for other silicon-based porous polymers.[15]
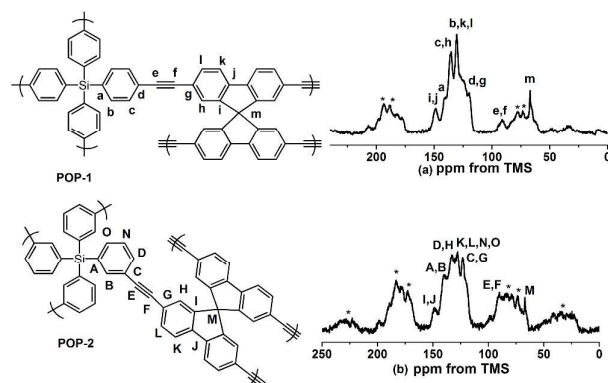

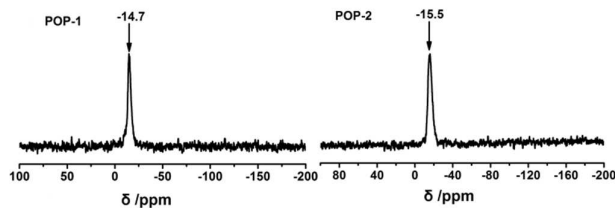**Fig. 2** Solid-state ^{13}C CP/MAS NMR spectra of POP-1 (a) and POP-2 (b)

Fig. 3 Solid-state ^{29}Si MAS NMR spectra of POP-1 and POP-2

Porosity

The porosities of the polymers were investigated by nitrogen sorption analysis at 77 K. Fig. 4a shows the N_2 adsorption-desorption isotherms of POP-1 and POP-2 and table 1 summarizes the porosity data of each polymer. All the polymers gave rise to type I N_2 isotherms with some type IV isotherm characteristics at higher relative pressure according to IUPAC classifications. All of the N_2 isotherms exhibited a

sharp uptake at relative low pressure and gradually increasing uptake at higher relative pressure with hysteresis to a degree, suggesting the presence of micropore and mesopore within the networks. The BET specific surface areas (S_{BET}) of POP-1 and POP-2 are 983 m^2 g^{-1} and 791 m^2 g^{-1}, respectively. The total pore volumes (V_{total}) of POP-1 and POP-2, estimated from the amount of N_2 adsorbed at $P/P_0 = 0.90$, are 0.81 cm^3 g^{-1} and 0.70 cm^3 g^{-1}, respectively. The pore size distributions (PSDs) were evaluated by nonlocal density functional theory (NL-DFT). These two polymers exhibited similar PSD curves with a narrow micropore distribution centered at 0.6 nm and 1.6 nm, and a relatively broad mesoprore with major diameters at 2.7 nm and 3.9 nm (Fig. 4b). The PSD results agreed with the shape of N_2 isotherms, suggesting that the structures featured micropores and mesopores. The contribution of microporosity to the polymers can be calculated from the ratios of micropore volume (V_{micro}) over V_{total}. The ratios V_{micro}/V_{total} of POP-1 and POP-2 are 0.14 and 0.10, further confirming the coexistence of micropore and mesopore within the networks.

On the basis of these results, POP-1 showed higher porosity than POP-2. This finding could be explained by the different structure geometry of the silicon-based monomers. In the case of POP-2, the kinked geometry of *m*-Si leads to a distorted network structure, resulting in decreased BET surface area and pore volume compared with those of POP-1 using *p*-Si as the monomer, which leads to a relatively less distorted structure that connects the spirobifluorene units. A similar relation between monomer structure and resulting porosity has also been found in other systems.[29,30] For example, Schwab *et al.* presented a series of cross-linked microporous polymers based on melamine and various di- or trialdehydes via Schiff base chemistry and found that SNW-3 based on *m*-phthaldialdehyde exhibited lower porosity than SNW-1 based on *p*-phthaldialdehyde.[29]

Table 1. Porosity data of POP-1 and POP-2

	S_{BET}[a]/m^2 g^{-1}	S_{micro}[b]/m^2 g^{-1}	V_{total}[c]/cm^3 g^{-1}	V_{micro}[d]/cm^3 g^{-1}	V_{micro}/V_{total}	S_{CO_2/N_2}	S_{CO_2/CH_4}	S_{CO_2/O_2}
POP-1	983	265	0.81	0.11	0.14	6.7	3.4	7.1
POP-2	791	169	0.70	0.073	0.10	11.8	4.8	13.0

[a] Surface area calculated from N_2 adsorption isotherm using the BET method; [b] Microporous surface area calculated from N_2 adsorption isotherm using *t*-plot method; [c] Total pore volume calculated at $P/P_0 = 0.90$; [d] Microspore volume derived using the *t*-plot method based on the Halsey thickness equation.

Compared to other porous polymers through the copolymerization reactions of spirobifluorene-based precursors and the second monomers (for clarify, spirobifluorene-containing monomers are considered as fundamental monomers, thus other monomers can be called the second monomers), herein the porosities of the polymers containing silicon-centered units are higher or comparable. For example, Yamamoto reaction of 2,2',7,7'-tetrabromo-9,9'-spirobifluorene (TBSF) with 1,4-dibromobenzene resulted in a network with a S_{BET} of 887 m^2 g^{-1},[22] which is lower than that of POP-1, but higher than that of POP-2. Thus these results

demonstrate that tetrahedral silicon-centered units could be introduced to the porous networks to increase their porosities, and copolymerization, i.e., altering the second monomer is an efficient strategy to tune the porous properties of the resultant polymers, consistent with previous reports.[31]
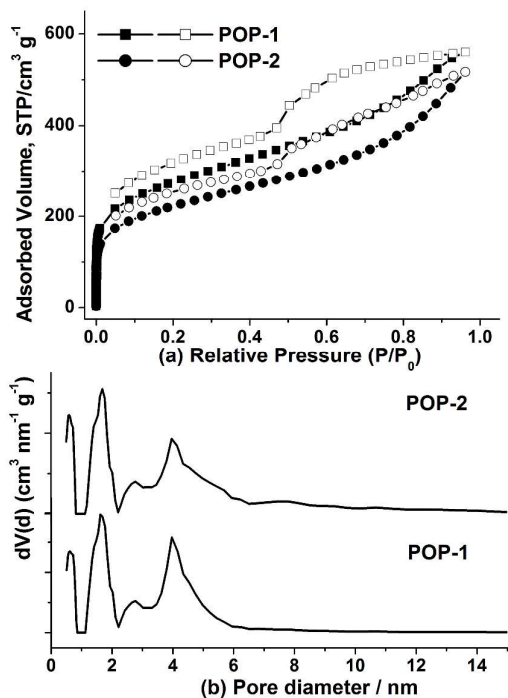
Fig. 4 (a) Nitrogen adsorption (closed symbols) and desorption (open symbols) isotherms for POP-1 and POP-2; (b) pore size distributions of POP-1 and POP-2 calculated by NL-DFT approach.

Thermal properties and morphology

To evaluate the thermal stability of these polymers, thermogravimetric analysis (TGA) was carried out in N_2 atmosphere at a heat rate of 10 °C min^{-1}. As shown in the Fig. 5, both POP-1 and POP-2 start to decompose at a high temperature up to 350°C (decomposition temperature at 5% mass loss), indicating that these polymers have excellent thermal stability, which is an essential merits for fabricating stable devices. POP-1 and POP-2 exhibit a similar decomposition trend with the temperature increasing. The final weight loss is low apparently due to the highly cross-linking networks.
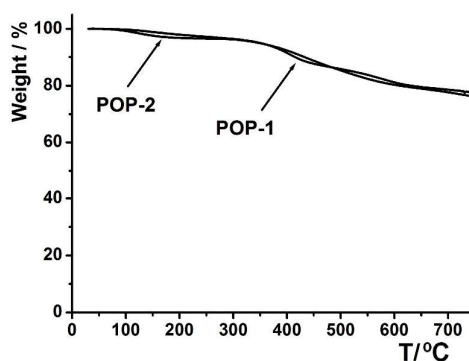

Fig. 5 TGA curves of POP-1 and POP-2 in nitrogen atmosphere

To observe the particle size and morphology, filed-emission scanning electron microscopy (FE-SEM) was performed. As

expected, these polymers showed similar morphology formed by inter-linking of irregular shapes with a wide range of size distribution from 100 nm to tens of micrometers (Fig. 6).
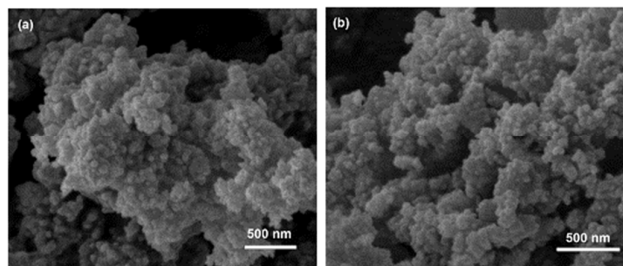

Fig. 6 FE-SEM image of POP-1 (a) and POP-2 (b)

CO_2 sorption and the selectivity of CO_2 over other gases

One important application of porous polymers is the capture and storage of CO_2 because CO_2 has been considered as the major contribution of global warming.[1-3,32-33] Therefore, we carried out CO_2 adsorption experiments at 273 K and 298 K to evaluate their potential applications in capturing and storing CO_2. For all materials, the CO_2 sorption was completely reversible and no significant hysteresis was observed (Fig.S1). POP-1 exhibited moderate CO_2 uptakes of 1.92 mmol g^{-1} (8.45 wt%) at 273 K and 1.03 bar, and 1.12 mmol g^{-1} (4.93 wt%) at 298 K and 1.01 bar (Fig. S1a). The uptakes of POP-2 were found to be 1.79 mmol g^{-1} (7.88 wt%) at 273 K and 1.03 bar, and 1.13 mmol g^{-1} (4.97 wt%) at 298 K and 1.02 bar, respectively (Fig. S1b). The slight decrease of CO_2 adsorption capacity for POP-2 than that for POP-1 was obviously due to the lower surface area. Their capacities were comparable to the corresponding values of some MOFs materials,[34] COFs materials,[35] and porous polymers[36] with a level of surface area, as well as some POP materials synthesized by Sonogashira-Hagihara reaction (e.g., CMP-1-(OH)$_2$, S_{BET}: 1043 m^2 g^{-1}, CO_2 uptake: 1.07 mmol g^{-1} at 298 K).[37] In fact, these capacities were even comparable to that reported for PAF-1 (S_{BET}: 5600 m^2 g^{-1}) despite having much lower surface areas.[13] However, these values are much less than some top-performing materials, such as ALP-1 (3.25 mmol g^{-1} at 298 K),[38] PPN-6-CH$_2$DETA (3.04 mmol g^{-1} at 295 K),[39] BILP-4 (2.98 mmol g^{-1} at 298 K),[40] and CPOP-1 (4.82 mmol g^{-1} at 273 K),[41] which could be attributed to the introduction of CO_2-philic functional groups in these materials.

The isosteric heat of adsorption (Q_{ST}) revealing the affinity between the network and CO_2, was calculated from the CO_2 isotherms collected at 298 K and 273 K employing the Clausius-Clapeyron equation. As shown in Fig. S1c, the adsorption enthalpy for these polymers was comparably high (26.8 kJ mol^{-1} and 25.2 kJ mol^{-1} for POP-1 and POP-2) at low coverage and gradually dropped at higher coverage, thereby indicating that the polymers possessed a high binding ability with CO_2. We speculate that these polymers absorbing CO_2 is based on a physisorption mechanism, unlike other POP materials containing CO_2-philic functional groups (e.g., amine groups) exhibiting both physisorption and chemisorption mechanism.[42]

Besides the loading capacity, another important factor for estimating how well the material will perform is the CO_2

ARTICLE

Journal Name

selectivity over other gases, including N_2, O_2 and CH_4, because exhaust gas (e.g., flue-gas from power stations) is a mixture of various gases for a realistic application.[43] Thus we also measured CH_4, N_2 and O_2 adsorption isotherms of POP-1 and POP-2 at low pressure at 298 K (Fig. 7). Then the selectivity (*S*) of CO_2 over other gases was calculated from the corresponding Henry's law constants.[44,45] A nonlinear fitting of the adsorption isotherms using the Toth model was performed (Fig. S2-S9) and the data were listed in Table 1. It is found that the values of CO_2/N_2, CO_2/CH_4 and CO_2/O_2 selectivity for POP-1 are 6.7, 3.4 and 7.1, while those for POP-2 are 11.8, 4.8 and 13.0 at 298 K. Compared to other POP materials, these values are moderate. For CO_2/N_2 selectivity, the values are comparable to several porous materials, such as MOF-508b (4),[46] ZIF-70 (17.3)[47] and some POP materials,[48] but obviously much lower than some top-performing materials, such as ALP-1 (27),[38] PPN-6-CH$_2$DETA (442),[39] BILP-4 (32),[40] and CPOP-1 (25),[41] due to the presence of CO_2-philic functional groups. For CO_2/CH_4 selectivity, the values are also comparable to many porous materials, such as Cu(BDC-OH) (6.7),[49] Zn$_4$(OH)$_2$(1,2,4-btc)$_2$ (4.5),[50] ALP-1 (5),[38] and BILP-4 (7).[40] For CO_2/O_2 selectivity, the values are higher than that of alumina (3.5). These results demonstrated that these porous materials could be potentially utilized as solid adsorbents for storing and capturing CO_2.
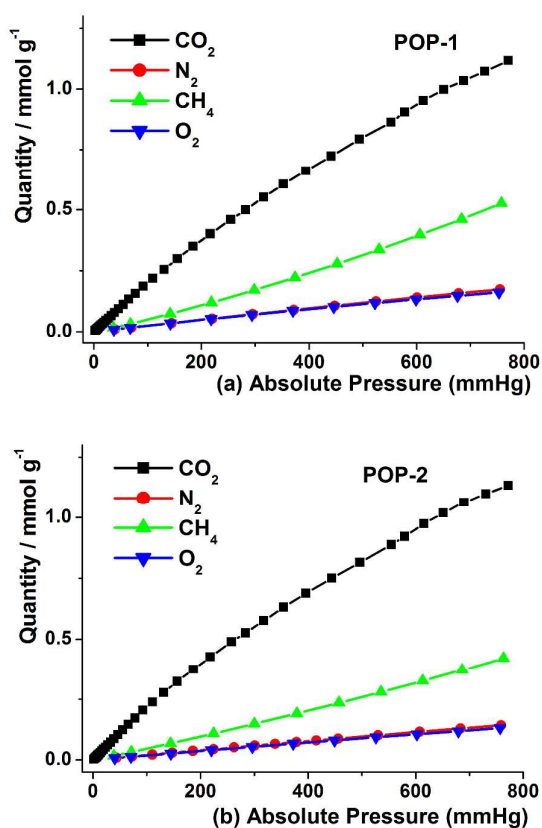

Fig. 7 CO_2, N_2, CH_4 and O_2 adsorption isotherms of POP-1 (a) and POP-2 (b) at 298 K

Conclusion

We have synthesized two novel porous organic polymers (POPs) simultaneously using tetrahedral silicon-centered monomers and stereocontorted spirobifluorene-based precursors as building units via Sonogashira-Hagihara coupling reaction. The resulting polymers exhibited high thermal stability, comparable high surface area with S_{BET} of up to 983 $m^2 g^{-1}$ and pore volume with V_{total} of up to 0.81 $cm^3 g^{-1}$. Their porosities could be tuned by altering the structure geometry of silicon-based monomers. Through further comparison with other porous polymers, the results revealed that tetrahedral silicon-centered monomers could be introduced to the porous networks to increase the porosity and copolymerization, i.e., altering the second monomer is an effective means to tune the porosity of the final products. Moreover, these materials exhibited moderate CO_2 capacities and moderate selectivity of CO_2 over other gases, including N_2, O_2 and CH_4, thereby revealing that they could be potentially applied in capturing and storing CO_2.

Notes and references

1   Y. Xu, S. Jin, H. Xu, A. Nagai, D. Jiang, *Chem. Soc. Rev.*, 2013, **42**, 8012–8031.
2   R. Dawson, A. I. Cooper and D. J. Adams, *Prog. Polym. Sci.*, 2012, **37**, 530–563.
3   D. Wu, F. Xu, B. Sun, R. Fu, H. He and K. Matyjaszewski, *Chem. Rev.*, 2012, **112**, 3959–4015.
4   A. Thomas, *Angew. Chem. Int. Ed.*, 2010, **49**, 8328–8344.
5   X. Du, Y. L. Sun, B. E. Tan, Q. F. Teng, X. J. Yao, C. Y. Sun and W. Wang, *Chem. Commun.*, 2010, **46**, 970–972.
6   A. I. Cooper, *Adv. Mater.*, 2009, **21**, 1291–1295.
7   J. X. Jiang, F. Su, A. Trewin, C. D. Wood, N. L. Campbell, H. Niu, C. Dickinson, A. Y.Ganin, M. J. Rosseinsky, Y. Z. Khimyak and A. I. Cooper, *Angew. Chem. Int. Ed.*, 2007, **46**, 8574–8578.
8   E. Stöckel, X. Wu, A. Trewin, C. D. Wood, R. Clowes, N. L. Campbell, J. T. A. Jones, Y. Z. Khimyak, D. J. Adams and A. I. Cooper, *Chem. Commun.*, 2009, **45**, 212–214.
9   S. Ren, R. Dawson, A. Laybourn, J.-X. Jiang, Y. Khimyak, D. J. Adams and A. I. Cooper, *Polym. Chem.*, 2012, **3**, 928–934.
10 A. Patra and U. Scherf, *Chem. Eur. J.*, 2012, **18**, 10074–10080.
11 J. H. Choi, K. M. Choi, H. J. Jeon, Y. J. Choi, Y. Lee and J. K. Kang, *Macromolecules*, 2010, **43**, 5508–5511.
12 J.-X. Jiang, A. Trewin, D. J. Adams and A. I. Cooper, *Chem. Sci.*, 2011, **2**, 1777–1781.
13 D. Yuan, W. Lu, D. Zhao and H.-C. Zhou, *Adv. Mater.*, 2011, **23**, 3723–3725.
14 M. F. Roll, J. W. Kampf, Y. Kim, E. Yi and R. M. Laine, *J. Am. Chem. Soc.*, 2010, **132**, 10171–10183.
15 D. Wang, W. Yang, L. Li, X. Zhao, S. Feng and H. Liu, *J. Mater. Chem. A*, 2013, **1**, 13549–13558.
16 T. Muller and S. Bräse, *RSC. Adv.*, 2014, **4**, 6886–6907.

Please do not adjust margins

RSC Advances

ARTICLE

17 T. Ben, H. Ren, S. Ma, D. Cao, J. Lan, X. Jing, W. Wang, J. Xu, F. Deng, J. M. Simmons, S. Qiu and G. Zhu, *Angew. Chem., Int. Ed.*, 2009, **48**, 9457–9460.

18 D. Wang, H. He, X. Chen, S. Feng, Y. Niu and D. Sun, *CrystEngComm,* 2010, **12**, 1041–1043.

19 J. R. Holst, E. Stöckel, D. J. Adams and A. I. Cooper, *Macromolecules*, 2010, **43**, 8531–8538.

20 M. Rose, W. Bohlmann, M. Sabo and S. Kaskel, *Chem. Commun.*, 2008, 2462–2464.

21 P. Kuhn, M. Antonietti and A. Thomas, *Angew. Chem. Int. Ed.*, 2008, **47**, 3450–3453.

22 J. Weber and A. Thomas, *J. Am. Chem. Soc.*, 2008, **130**, 6334–6335.

23 J. Schmidt, M. Werner and A. Thomas, *Macromolecules*, 2009, **42**, 4426–4429.

24 H. Ren, Q. Tao, Z. Gao, Di Liu, *Dyes Pigments*, 2012, **94**, 136–142.

25 D. Wang, Y. Niu, Y. Wang, J. Han, S. Feng, *J. Organomet. Chem.*, 2010, **695**, 2329–2337.

26 X. Zhao, L. Zhang, H. Ma, D. Sun, D. Wang, S. Feng and D. Sun, *RSC Adv.*, 2012, **2**, 5543–5549.

27 J. X. Jiang, F. Su, A. Trewin, C. D. Wood, H. Niu, J. T. A. Jones, Y. Z. Khimyak and A. I. Cooper, *J. Am. Chem. Soc.*, 2008, **130**, 7710–7720.

28 B. Kiskan, M. Antonietti and J. Weber, *Macromolecules*, 2012, **45**, 1356–1361.

29 25. M. G. Schwab, B. Fassbender, H. W. Spiess, A. Thomas, X. Feng and K. Müllen, *J. Am. Chem. Soc.*, 2009, **131**, 7216–7217.

30 K. V. Rao, S. Mohapatra, C. Kulkarni, T. K. Maji and S. J. George, *J. Mater. Chem.*, 2011, **21**, 12958–12963.

31 M. Yu, X. Wang, X. Yang, Y. Zhao and J.-X. Jiang, *Polym. Chem.*, 2015, **6**, 3217–3223.

32 G. Férey, C. Serre, T. Devic, G. Maurin, H. Jobic, P. L. Llewellyn, G. D. Weireld, A. Vimont, M. Daturi and J.-S. Chang, *Chem. Soc. Rev.*, 2011, **40**, 550–562.

33 Y.-S. Bae and R. Q. Snurr, *Angew. Chem., Int. Ed.*, 2011, **50**, 11586–11593.

34 A. Mallick, S. Saha, P. Pachfule, S. Roy and R. Banerjee, *J. Mater. Chem*., 2010, **20**, 9073–9080.

35 T. Fröschl, U. Hörmann, P. Kubiak, G. Kučrová, M. Pfanzelt, C. K. Weiss, R. J. Behm, N. Hüsing, U. Kaiser, K. Landfester and M. Wohlfahrt-Mehrens, *Chem. Soc. Rev.*, 2012, **41**, 5313–5360.

36 R. Dawson, E. Stöckel, J. R. Holst, D. J. Adams and A. I. Cooper, *Energy Environ. Sci.*, 2011, **4**, 4239–4245.

37 R. Dawson, D. J. Adams and A. I. Cooper, *Chem. Sci.*, 2011, **2**, 1173–1177.

38 P. Arab, M. G. Rabbani, A. K. Sekizkardes, T. İslamoğlu and H. M. El-Kaderi, *Chem. Mater.*, 2014, **26**, 1385–1392.

39 W. Lu, J. P. Sculley, D. Yuan, R. Krishna, Z. Wei and H.-C. Zhou, *Angew. Chem. Int. Ed.*, 2012, **51**, 7480–7484.

40 M. G. Rabbani and H. M. El-Kaderi, *Chem. Mater.*, 2012, **24**, 1511–1517.

41 Q. Chen, M. Luo, P. Hammershøj, D. Zhou, Y. Han, B. W. Laursen, C.-G. Yan and B.-H. Han, *J. Am. Chem. Soc.*, 2012, **134**, 6084–6087.

42 B. Dutcher, M. Fan and A. G. Russell, *ACS Appl. Mater. Interfaces*, 2015, **7**, 2137–2148.

43 D. M. D'Alessandro, B. Smit and J. R. Long, *Angew. Chem. Int. Ed.*, 2010, **49**, 6058–6060.

44 E. Neofotistou, C. D. Malliakas, P. N. Trikalitis, *Chem. Eur. J.*, 2009, **15**, 4523–4527.

45 B. Wang, A. P. Côté, H. Furukawa, M. O'Keeffe, O. M. Yaghi, *Nature*, 2008, **453**, 207–211.

46 L.Bastin, P. S. Barcia,E. J.Hurtado, J. A. C. Silva, A. E. Rodrigues and B. Chen, *J. Phys. Chem. C*, 2007, **112**, 1575–1581.

47 A. Phan, C. J. Doonan, F. J. Uribe-Romo, C. B. Knobler, M. O'Keeffe and O. M. Yaghi, *Acc. Chem. Res.*, 2010, **43**, 58–67.

48 V. Guillerm, Ł. J. Weseliński, M. Alkordi, M. I. H. Mohideen, Y. Belmabkhout, A. J. Cairns and M. Eddaoudi, *Chem. Commun.*, 2014, **50**, 1937–1939.

49 Z. X. Chen, S. C. Xiang, H. D. Arman, P. Li, S. Tidrow, D. Y. Zhao and B. L. Chen, *Eur. J. Inorg. Chem.*, 2010, 3745–3749.

50 J. R. Li, Y. G. Ma, M. C. McCarthy, J. Sculley, J. M. Yu, H. K. Jeong, P. B. Balbuena and H. C. Zhou, *Coord. Chem. Rev.*, 2011, **255**, 1791–1823.